Available online at www.sciencedirect.com
SCIENCE DIRECT
Thermochimica Acta 437 (2005) 168–178
thermochimica acta
www.elsevier.com/locate/tca

A study on the thermal decomposition behavior of derivatives of 1,5-diamino-1*H*-tetrazole (DAT): A new family of energetic heterocyclic-based salts

Gerd Fischer [a], Gerhard Holl [b], Thomas M. Klapötke [a,*], Jan J. Weigand [a]

[a] *Department of Inorganic Chemistry, Ludwig-Maximilian University of Munich, D-81377 Munich, Germany*
[b] *Bundeswehr Research Institute for Materials, Fuels and Lubricants, Swisttal-Heimerzheim, Großes Cent, D-53913 Swisttal, Germany*

Received 4 February 2005; received in revised form 2 May 2005; accepted 8 June 2005
Available online 2 August 2005

Abstract

The thermal decomposition of the highly energetic 1,5-diamino-4-methyl-1*H*-tetrazolium nitrate (**2b**), 1,5-diamino-4-methyl-1*H*-tetrazolium dinitramide (**2c**) and 1,5-diamino-4-methyl-1*H*-tetrazolium azide (**2d**) were investigated by thermogravimetric analysis (TGA) and differential scanning calorimetry (DSC). Mass spectrometry and IR spectroscopy were used to identify the gaseous products. Decomposition appears in the cases of **2c** and **2d** to be initiated by a proton transfer to form the corresponding acid HN_3 and HN_3O_4 whereas in the case of **2b** a methyl group transfer to $MeONO_2$ is observed as initial process. The gaseous products after the exothermic decomposition are comparable and are in agreement of the possible decomposition pathways discussed for the corresponding compounds. For all processes, possible decomposition schemes are presented. The decomposition temperatures of **2b** and **2c** are significantly higher than that of **2d** and were supported by evaluation the values of the activation energy according the method of Ozawa and Kissinger.

Keywords: Energetic tetrazolium salts; Thermal stability; Thermal decomposition; IR spectroscopy; Mass spectrometry

1. Introduction

We are currently investigating the chemistry of tetrazole derivatives with respect to the continuous interest in high-nitrogen compounds as ingredients for propellants and explosives [1–4]. Among those high nitrogen compounds, the nitrate, dinitramide and azide salts have received major attention as from the energetic point of view, desirable properties of energetic materials are a high oxygen balance (nitrates and dinitramide salts), a high heat of formation $\Delta_f H^\circ$, the release of high amounts of gases (e.g. N_2) as favored explosion products and high values of the density ρ. Although the highest densities are obtained for crystal structures of neutral molecules (e.g. CL-20 ($\rho = 2.04\,g\,cm^{-3}$) [5], TNAZ ($\rho = 1.85\,g\,cm^{-3}$) [6] and TEX ($\rho = 1.99\,g\,cm^{-3}$) [7]), the search for high energy salts is of great interest, as in most cases the preparations of those salts are very easy, since they mostly involve simple acid-base or metatethical reactions. Nitrates [8,9], for example, are powerful oxidizing agents and decompose at elevated temperatures to give oxygen as one of the major products. Extensive studies have been made on the syntheses, thermal properties and sensitivities of, e.g. ammonium nitrate (AN) [10,11], dinitramide salts [12–17] and azides [18–20]. Most of these salts are water soluble and highly hygroscopic but compounds which are neither soluble in water nor hygroscopic and having a very low sensitivity are required.

Aminotetrazoles are heterocycles, rich in electron pairs. The reaction with strong acids leads in the case of 1,5-diamino-1*H*-tetrazole (**1**) (e.g. $X^- = NO_3$, ClO_4) [21,22] to the formation of the corresponding salts (**1a** and **1b**, Fig. 1).

* Corresponding author. Tel.: +49 89 2180 77491/77497; fax: +49 89 2180 77492.
E-mail address: tmk@cup.uni-muenchen.de (T.M. Klapötke).

0040-6031/$ – see front matter © 2005 Elsevier B.V. All rights reserved.
doi:10.1016/j.tca.2005.06.034

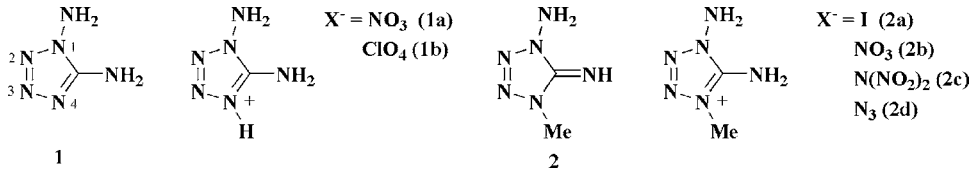

Fig. 1. Derivatives of 1,5-diamino-1*H*-tetrazole (**1**).

However, the protonation of **1** can proceed both on the nitrogen atoms of the tetrazole ring and on the amino group(s) and was determined to proceed unambiguously at the N4 atom of the ring (Fig. 1) [23]. Not much is known about corresponding azide or dinitramide salts and we have not succeeded in finding any references in literature concerning the isolation of those salts. In ref. [24,25], we summarized our observation of the protonation of 1,5-diamino-1*H*-tetrazole **1** with nitric and perchloric acid (**1a** and **1b**) and introduced a new derivative of **1**, the 1-amino-4-methyl-5-imino-4,5-dihydro-1*H*-tetrazole **2** as its iodide (**2a**), nitrate (**2b**), dinitramide (**2c**) and azide (**2d**) salt. By the formal exchange of the proton by a methyl group we expected a lower acidity, hence a higher stability of the corresponding azide (**2d**) and dinitramide (**2c**) salt. This paper presents fundamental properties (crystal densities), sensitivity (friction, impact, TGA and DSC) data and the thermal behavior of **2b**, **2c** and **2d** by a study of the thermal decomposition and the determination of the decomposition products by means of IR gas phase analysis and mass spectrometry.

2. Experimental

2.1. Caution

The salts **2c** and **2d** are energetic materials and appropriate safety precautions should be taken, especially when these compounds prepared on a larger scale. Laboratories and personnel should be properly grounded and safety equipment such as Kevlar® gloves, leather coat, face shield and ear plugs are necessary when manipulating these salts.

1,5-Diamino-4-methyl-1*H*-tetrazolium nitrate (**2b**), 1,5-diamino-4-methyl-1*H*-tetrazolium dinitramide (**2c**) and 1,5-diamino-4-methyl-1*H*-tetrazolium azide (**2d**) were synthesized according to ref. [25]. Properties of these salts are listed in Table 1. The thermal stability was initially evaluated using differential scanning calorimetry (DSC) and thermogravimetric analysis (TGA). For initial safety testing, the impact and friction sensitivity was tested according to BAM methods with the "BAM Fallhammer" and "BAM friction tester" [26]. DSC measurements were carried out as follows. Samples (∼1 mg) were analyzed in closed Al-containers with a hole (1 μm) on the top for gas release with a nitrogen flow of 20 mL/min and a heating rate of $\beta = 10\,^{\circ}$C/min. The reference sample was an Al-container with air.

Experiments were carried out from 50–400 °C. The sample and the reference pan were heated in a differential scanning calorimeter (Perkin-Elmer Pyris 6 DSC, calibrated by standard pure Indium and Zinc). Compounds **2b**, **2c** and **2d** were also subjected to TGA analysis in a nitrogen atmosphere in open Al_2O_3 crucibles (sample weight ∼1 mg) at a heating rate of $\beta = 10\,^{\circ}$C/min with a thermogravimetric analyzer (Setaram DTA-TGA 92) in the temperature range from 50–400 °C. For the removal of moisture, all samples were dried in vacuo for 24 h at 40 °C. The energy of activation for the decomposition step was estimated by the method of Ozawa [28] and Kissinger [29] by following the differential heating rate method of the American Society for Testing and Materials (ASTM) according to the ASTM protocol E 698–99 [30]. Thermograms were collected by analyzing samples (∼0.3 mg) in closed Al-containers with a nitrogen flow of 20 mL/min. The reference sample was an Al-container with air. The sample size was kept small to minimize temperature gradients within the sample and a 0.003 × 3/16-in. disk was used to optimize good thermal contact between the sample and container (according ASTM E 698–99). Also the volatility of the compounds used was taken into account by testing the samples using a sealed hermetic container to prevent interferences from vaporization and weight loss of

Table 1
Properties of salts **2b**, **2c** and **2d**

	Formula	Ω[a] (%)	ρ[b] (g/cm^3)	P[c] (GPa)	D[c] (m s^{-1})	Impact[d] (kg cm); (Nm)	Friction[e,f]	$\Delta_f H°$[g]
2b	$(C_2H_7N_6)^+NO_3^-$	−40.6	1.506	23.4	7682	>200 (>40 J)	120 N (−)	+174.5
2c	$(C_2H_7N_6)^+N(NO_2)_2^-$	−25.3	1.719	33.6	8827	70 (7 J)	20 N (+)	+385.3
2d	$(C_2H_7N_6)^+N_3^-$	−76.4	1.417	20.8	7405	150 (15 J)	192 N (−)	+676.1

[a] Oxygen balance.
[b] Calculated density from X-ray structure.
[c] Calculated detonation pressures (P) and detonation velocities (D) using the semi-empirical equations suggested by Kamlet and Jacobs, see ref. [27].
[d] Insensitive >40 J, less sensitive ≥35 J, sensitive ≥4, very sensitive ≤3 J.
[e] Insensitive >360 N, less sensitive = 360 N, sensitive <360 N and >80 N, very sensitive ≤80 N, extreme sensitive ≤10 N.
[f] According to the UN recommendations on the transport of dangerous goods, (+) indicates: not safe for transport.
[g] Calculated molar enthalpy of formation in kJ mol^{-1} using G2 method, see ref. [25].

unreacted material. We found that for our requirements the use of a hermetic container was necessary to obtain a good estimate of the activation energy. Experiments were carried out from 30–350 °C at different heating rates of $\beta = 2$, 5, 10, 15, 20 and 40 °C for **2b** and **2c** and $\beta = 10$, 15, 20, 40 and 50 °C/min for **2d**. We assume that the rate constant follows the Arrhenius law and that the exothermic reaction can be considered as a single step; certainly the conversion at the maximum rate is independent of the heating rate, when this is linear. In order to get a better agreement of the activation energies determined according the Kissinger and Ozawa method, following the ASTM protocol, a refinement of the Kissinger activation energy (1)

$$E_a = -2.19R\left[\frac{d(\log_{10}\beta)}{d(1/T)}\right] \quad (1)$$

according to (2)

$$E_a = \left(-2.303\frac{R}{D}\right)\left[\frac{d(\log_{10}\beta)}{d(1/T)}\right] \quad (2)$$

using given D factors in [30] leads to very close agreements.

In order to analyse the gases from the stepwise decomposition of the compounds, a specially equipped IR-cell was loaded with the compounds (~2 mg) and evacuated. The sample holder of the IR cell was heated at a rate of 4 °C/min (CARBOLITE 900 °C Tube Furnace type MTF 9/15) and the reaction products were allowed to expand continuously into the gas cell. During this heating, the IR-spectra were recorded continuously as a function of the heating rate using a Perkin-Elmer Spektrum One FT-IR instrument. To record the mass spectra, a sample (~1 mg) of the corresponding compound was heated at a heating rate of 4 °C/min (CARBOLITE 900 °C Tube Furnace type MTF 9/15) in a one side closed glass tube (length: 500 mm; diameter: 5 mm) connected to the reservoir of the mass spectrometer (JEOL MStation JMS 700). In this case, the spectra were also recorded as a function of the heating rate. Residual decomposition products (e.g. sublimed material and residue after the decomposition) were identified by means of mass spectrometry (EI and DEI mode) and NMR (^{1}H, ^{13}C) techniques. The ^{1}H and ^{13}C spectra were recorded on a JEOL Eclipse 400 instrument in [d6]-DMSO, and chemical shifts were referenced to TMS. Reference data for **1** and **2** were obtained from authentic samples and in the case of **6**, **13** and **14** from [31].

In order to identify the decomposition gases, the sample was sealed under vacuum and heated to complete decomposition. The decomposition gases were then analyzed by IR spectroscopy (gas phase spectra) and mass spectrometry (JEOL MStation JMS 700) using electron impact (EI) mode (mass range 10–200; 0.5 scans per second, 70 eV).

3. Results and discussion

The reaction of 1,5-diamino-1*H*-tetrazole (**1**) with iodomethane followed by the metatethical reaction of the iodide (**2a**) with silver nitrate (**2b**), silver dinitramide (**2c**) or silver azide (**2d**) leads to a new family of heterocyclic-based salts. In all cases, stable salts were obtained and fully characterized by vibrational (IR, Raman), multinuclear NMR spectroscopy, mass spectrometry, elemental analysis, X-ray structure determination, as well as initial safety testing (impact and friction sensitivity) [25]. Preliminary sensitivity testing of the crystalline compounds indicates for all compound rather low impact sensitivities with the highest for the dinitramide (**2c**) with a value of 7 J in contrast to its relatively high friction sensitivity of 24 N. The nitrate (**2b**, 120N) and azide (**2d**, 54 N) have a comparable or lower friction sensitivity than RDX (120 N) (Table 1). For the compounds **2b**, **2c** and **2d**, the calculated detonation pressures lies in the range of $P = 20.8$ GPa (**2d**, comparable to TNT [32], $P = 20.6$ GPa) to $P = 33.6$ GPa (**2c**, comparable to RDX [32], $P = 34.4$ GPa) and detonation velocities in the range of $D = 7405\ m\ s^{-1}$ (**2d**, comparable to nitroglycerin [33], $D = 7610\ m\ s^{-1}$) to $D = 8827\ m\ s^{-1}$ (**2c**, comparable to RDX [33], $D = 8750\ m\ s^{-1}$) and correlate well with the increase of the density (**2d** (1.417) < **2b** (1.506) < **2c** (1.719)). The oxygen balance of these salts ranging from −76.4% to −25.3%. The heats of combustion for the investigated compounds were determined experimentally and the heats of formation were calculated by following a designed Born–Haber energy cycle [25]. The heats of formation were found to be positive with the highest for **2d** (676.1 kJ mol^{-1}). Also **2d** shows higher sensitivities toward friction and impact, the predicted detonation performance is higher than those found for ADN [14]. According to the UN guidelines ST/SG/AC.10/11 [34] a substance is considered to be too dangerous to be transported in the form in which it was tested if the friction load is less than 80 N or if the impact energy is 2 J or less at a probability of 16.7% (one of six).

3.1. Kinetics

DSC and TGA were used to evaluate the relative thermal stabilities of **2b**, **2c** and **2d** and are measured under comparable condition (Al-containers with a hole (1 μm) on the top for gas release for DSC measurements). Figs. 2–4 show the obtained DSC and TGA thermographs of these salts. All three compounds have relatively low melting points (**2b**, mp 121 °C (onset); **2d**, 135 °C (onset)), with the lowest for the dinitramide salt (**2c**, 85 °C (onset)) and start to decompose in the range of 175–250 °C (**2b**), 150–230 °C (**2c**) and 137–310 °C (**2d**). The enthalpy of melting, $\Delta_m H$, were found to be 122 (**2b**), 118 (**2c**) and 181 (**2d**) J g^{-1} (Table 2).

2b shows three main signals which can be related to the melting, first endothermic signal, the main decomposition reaction (second exothermic signal) and third exothermic signal, which corresponds to condensation reaction of the residual fragments of the exothermic step. In the case of the azide **2d**, two endothermic steps indicate a marked degree of sublimation around the melting temperature together with the start of the decomposition. Repeating the experiment with a

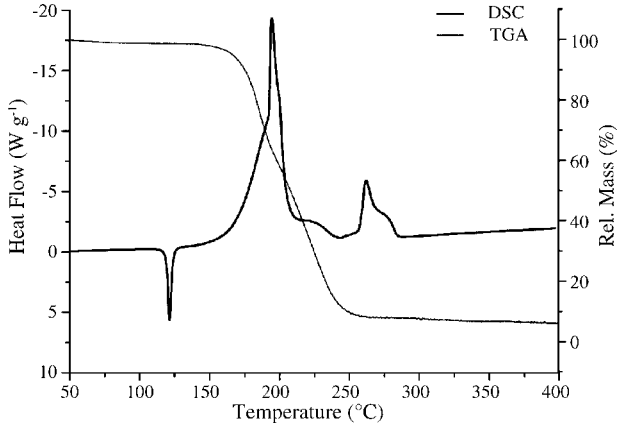

Fig. 2. DSC and TGA thermographs of **2b** ($\beta = 10\,^{\circ}$C/min).

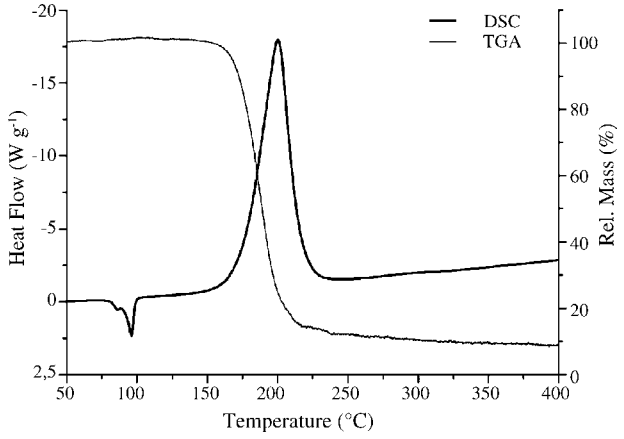

Fig. 3. DSC and TGA thermographs of **2c** ($\beta = 10\,^{\circ}$C/min).

closed Al-container with the same heating rate resulted in the coalescence of the two endothermic signals into one signal. The main decomposition step of **2d** is found in the region of 160–220 °C and, comparable to **2b**, the weak exothermic

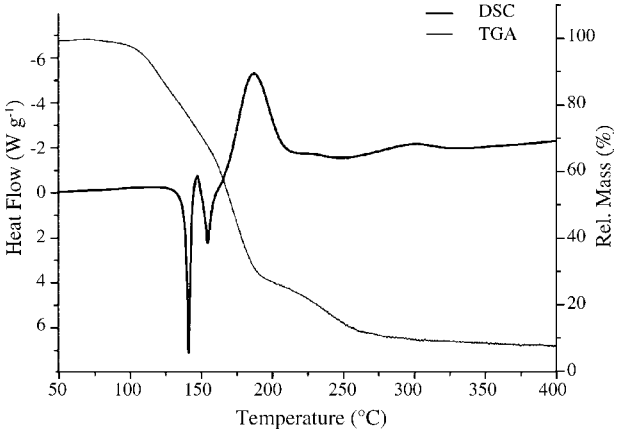

Fig. 4. DSC and TGA thermographs of **2d** ($\beta = 10\,^{\circ}$C/min).

region (275–325 °C) also corresponds to condensation reactions of residual fragments of the decomposition step. The DSC curves of the investigated **2c** is divided into three parts, the first one corresponds to a phase transition region which appears as one small endothermic reaction ($T_g = 82\,^{\circ}$C), the second part shortly after, is related to the melting region of **2c** as a endothermic peak. The third exothermic peak corresponds to the decomposition reaction. The purities of the compounds were determined to be higher than 98% by the evaluation of the corresponding melting peaks with the van't Hoff equation according ASTM protocol E 928–96 [35].

All three salts do not decompose residual free in the temperature range of 50–400 °C, as the mass loss in all case was determined by TGA to be ~90% (Table 2). The reason for this is found in the formation of condensation products with higher molecular mass, e.g. melam, melem or melom [36]. These products decompose at higher temperatures (>500 °C) to volatile substances like cyanamide, hydrogen cyanide and ammonia [37]. According to the mass loss derived from the TGA experiment, the dinitramide salt (**2c**) decomposes in one

Table 2
Properties of the salts **2b**, **2c** and **2d** related to the DSC and TGA measurements

	T_m[a] (°C)	$\Delta_m H$[b] (J g^{-1})	T_d[c] (°C)	T_{int}[d] (°C)	$\Delta_{max} H$[e] (J g^{-1})	Purity[f]	Mass loss[g]
2b	121	122	181	185–250	2085	>99%	33% (150–195 °C) 58% (195–275 °C)
2c	85 (T_g 82 °C)[h]	118	184	150–230	2823	>98%	90% (150–250 °C)
2d	133 (133)[i]	181[j] (171)[k]	137	137–310	916	>98%	34% (105–160 °C) 36% (160–185 °C) 19% (185–310 °C)

[a] Melting point (onset) from DSC experiment ($\beta = 10\,^{\circ}$C min^{-1}).
[b] Enthalpy of melting.
[c] Decomposition temperature (onset) from DSC experiment ($\beta = 10\,^{\circ}$C min^{-1}).
[d] Range of decomposition.
[e] Heat of combustion from maximum exothermic step.
[f] According the ASTM protocol E 928–96.
[g] From TGA experiment ($\beta = 10\,^{\circ}$C min^{-1}).
[h] Onset of phase transition.
[i] Melting point (onset) from DSC experiment ($\beta = 10\,^{\circ}$C min^{-1}) in closed Al-container (°C).
[j] Indicating a marked degree of sublimation around the melting temperature together with the start of the decomposition.
[k] Enthalpy of melting (J g^{-1}) determined in closed Al-container.

Table 3
Maximum exothermic responses of **2b**, **2c** and **2d** as a function of scan speed

S. no.	β (°C/min)	T_p (°C)	E_a (kJ mol^{-1}) Ozawa [28]	E_a (kJ mol^{-1})[a] Kissinger [29]
2b				
1	2	176.55	130.04 ± 3.68	130.08 ± 3.43
2	5	186.58		
3	10	195.56		
4	20	205.48		
5	40	216.09		
2c				
1	2	177.12	137.61 ± 4.52	137.70 ± 4.23
2	5	186.44		
3	10	195.23		
4	20	204.03		
5	40	214.64		
2d				
1	10	185.14	107.32 ± 4.18	107.61 ± 3.77
2	15	190.93		
3	20	194.85		
4	30	201.13		
5	50	211.04		

[a] Refined Kissinger activation energy according ASTM E 698–99 [30].

Table 4
Observed mass (*m*/*z*) in the decomposition experiments of **2b**, **2c** and **2d**

m/*z*	**2b**	**2c**	**2d**	
126	x	x	x	$(H_2NCN)_3$
81	x	x		$(HCN)_3$
69	x	x	x	1,2,4-Triazole
57	x	x	x	MeN_3, H_2NNCNH
56		x		
54	x			$(HCN)_2$
46	x			$MeONO_2$[a]
44	x	x		CO_2, N_2O
43			x	HN_3
42			x	H_2NCN
32	x			CH_3OH
30	x	x		NO, H_2CO
29			x	
28	x	x	x	CO, N_2
27	x		x	HCN
18	x	x		H_2O
17	x	x		NH_3
15			x	
14	x	x	x	

[a] Mass peak not observed.

single step, whereas in the case of **2b**, two decomposition steps are determined and in the case of **2d** three (Table 2). A closer inspection of the decomposition products of these salts reveals in all cases comparable decomposition pathways.

Differential scanning calorimetric studies have been carried out at five different heating rates (Table 3) to calculate the energy of activation by following the methods according the ASTM protocol [30]. It is observed that the temperature of decomposition increases with the increased heating rate of heating of the sample. The calculated activation energy values are in the case of **2b** and **2c** comparable and have been found to be 130.1 kJ mol^{-1} (**2b**, Ozawa) and 137.7 kJ mol^{-1} (**2c**, Ozawa), respectively. Compared to this, the activation energy of **2d** was found to be 111.7 kJ mol^{-1} (Ozawa). The activation energy values suggest that **2d** is more thermally labile than **2b** and **2c** indicating a different decomposition pathway, when compared in terms of calculated activation energies. The refined values of the activation energy obtained according the Kissinger method show an excellent correlation (Table 3).

3.2. Decomposition experiments

The typical products detected during the decomposition of the azide **2d** (by means of IR and mass spectrometry) are HN_3 (*m*/*z* 43), NH_4N_3, HCN (*m*/*z* 27), NH_3 (*m*/*z* 17), MeN_3 (*m*/*z* 57), N_2 (*m*/*z* 28) and traces of 1,2,4-triazole (*m*/*z* 69) (Table 4). Two distinctive temperature regimes have been identified for the decomposition of **2d**. As it is typical for ammonium salts of hydrazoic acid, the release of HN_3 starts at comparable low temperature and in the case of **2d**, the appearance of HN_3 in the IR spectra was already observed at about 60 °C (Fig. 5). This is not consistent with the TGA experiment where this temperature was determined to be ∼105 °C. One explanation for this observation is that the thermodynamic conditions for both experiments are different with respect to pressure. The IR experiment was carried out by thermal heating with a pressure of 5 μbar, whereas the TGA experiments had nitrogen as purge gas (20 cm^3/min). The mass loss of the first step was determined to be ∼34% which is in excellent agreement with the reaction process shown in Scheme 1 for the first step, the release of HN_3.

The 1-amino-4-methyl-5-imino-4,5-dihydro-1*H*-tetrazole (**2**) which remains after the evolution of the HN_3 decomposes under thermal stress to methyl azide (**3**) and the aminocyanamide (**4**) and also this process coincidences well with the observed mass loss of 36% (Table 2, Scheme 1, **I**) for the second step. In accordance with the observation of Levchick et al. [38] the trimerization product of **4**, 2,4,6-trihydrazino-1,3,5-triazine (**5**), was not detected as it is unstable at high temperatures and partially decomposes

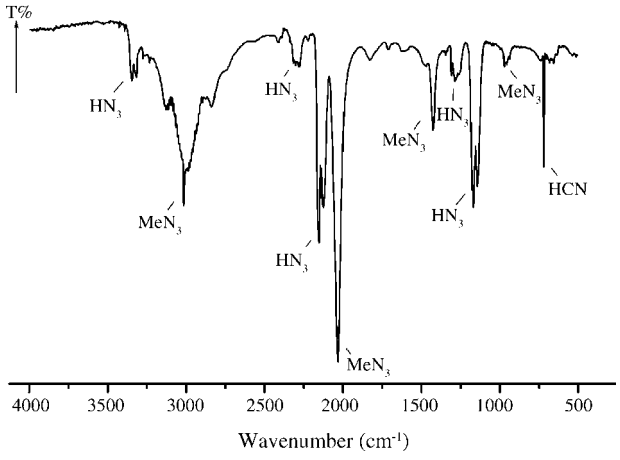

Fig. 5. Gas phase IR spectrum of the decomposition products of **2d**.

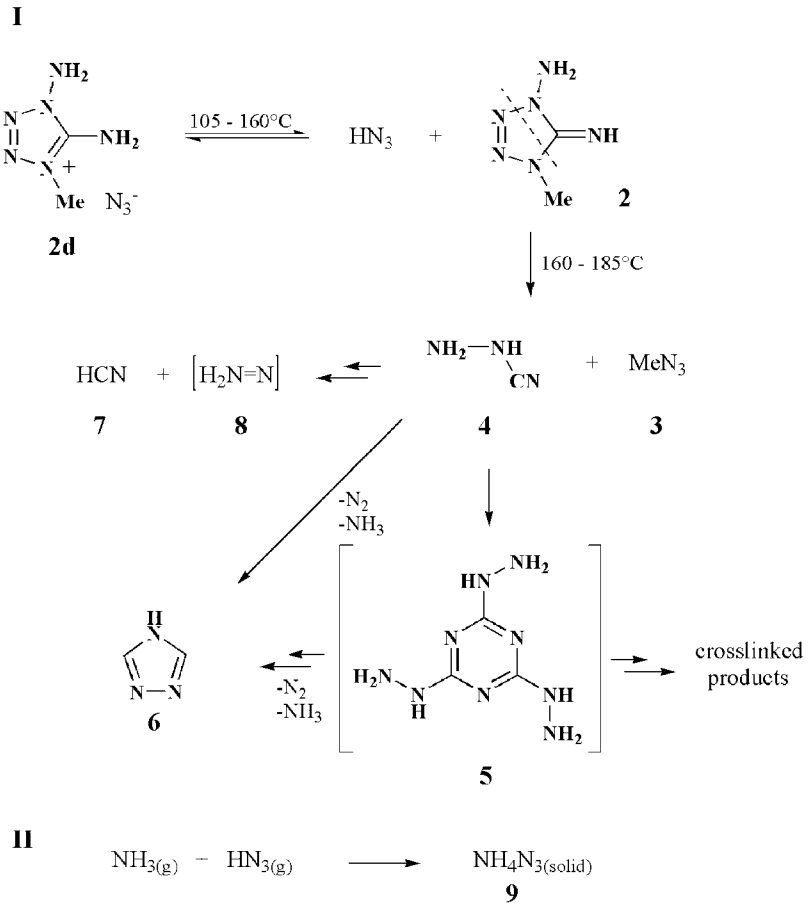

Scheme 1. Proposed decomposition pathway of **2d**.

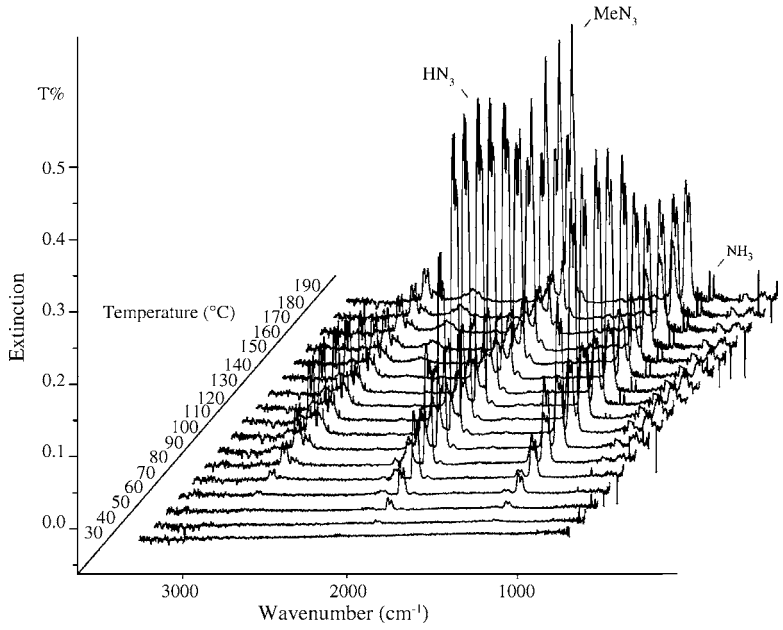

Fig. 6. Infrared spectroscopic evolved gas analysis of **2d**.

under ring-narrowing with the formation of 1,2,4-triazole (**6**) [39,40].

In the small amount of solid residue of the decomposition experiments, triazine structures crosslinked by –NH– could be identified by means of IR spectroscopy. The thermal decomposition residues after the third stage of weight loss (∼10%) have IR spectra similar to those of the products of thermal decomposition of 5-aminotetrazole, showing characteristic absorptions (3400–3100, 1670–1350, 810 and 780 cm^{-1}) of condensed cross-linked melamine derivatives [41,42]. The other possible decomposition route of 4 is the decomposition to HCN (**7**) under the formation of the corresponding unstable nitrene (**8**). **7** was also identified in the IR spectrum of the explosion products of **2d** (Fig. 5).

The TGA results are also in very good agreement with stepwise decomposition determined by IR spectroscopy. The identification of the decomposition gases allows the evaluation of the chemical processes during the thermal degradation of **2d**. Fig. 6 show those decomposition gases detected by IR spectroscopy and released during heating of **2d** from 30 to 190 °C. Ammonium azide (**9**) is produced from the recombination of ammonia NH_3 and HN_3, which is subsequently produced during the decomposition of **2d** and illustrates the descent of the intensities of the bands of HN_3 in the IR spectra (Scheme 1, **II**, Fig. 6) at temperatures higher than 150 °C. **9** was identified in the obtained sublimate. The mechanism for the decomposition of **2** becomes predominant as indicated by the increasing band around 2050 cm^{-1} which belongs to MeN_3 (**3**) (Fig. 6).

The vibrational frequencies of the experimentally observed IR-active gases are summarized in Table 5.

Table 5
Vibrational frequencies (cm^{-1}) of the experimentally observed molecules in the gas phase

Species	Frequencies	Reference
HN_3	3336 (m), 2140 (vs), 1264 (m), 1151 (vs), 607 (w), 607 (vw)	[49]
MeN_3	2940 (m), 2818 (w), 2539 (vw), 2198 (s), 2104 (vs), 1466 (vw), 1450 (vw), 1284 (s), 920 (w), 676 (w)	[50]
NH_3	3336 (m), 1626 (s), 968 (vs), 933 (vs)	[51]
HCN	3311 (s), 2097 (w), 712 (vs)	[49]
$MeONO_2$	2959 (m), 2917 (m), 1678 (vs), 1661 (vs), 1442 (m), 1430 (m), 1296 (s), 1287 (s), 1278 (s), 1017 (s), 862 (s), 855 (s), 853 (s), 844 (s) 758 (m), 658 (m)	[52]
N_2O	3891 (w), 3480 (m), 2809 (w), 2591 (m), 2488 (m), 2457 (vs), 2217 (vs), 1890 (w), 1302 (vs), 1275 (vs), 1183 (m), 1155 (m), 694 (w), 588 (w)	[53,54]
CO_2	3716 (w), 3609 (w), 2326 (vs), 741 (m), 667 (vs)	[55]
CO	2179 (vs), 2114 (vs)	[55]
H_2O	3657 (s), 1595 (s)	[51]

The thermal decomposition of **2b** under reduced pressure in the temperature of 140–300 °C is shown in Fig. 7. **2b** melts at 121 °C and the melt is stable up to 190 °C where shortly after, in accordance to the DSC experiment, decomposition occurs and a broad exothermic peak in the DSC and a sudden rise of gaseous products in the IR spectra indicates a spontaneous decomposition. In comparison to AN, **2b** shows a comparable decomposition region of ∼185–250 °C (AN 210 °C and 260 °C) which leads in contrast to AN to the for-

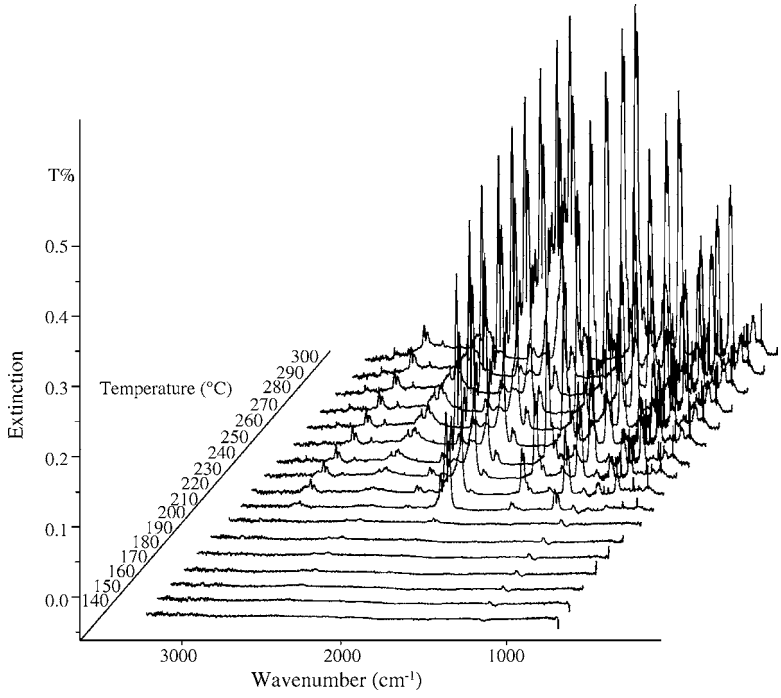

Fig. 7. Infrared spectroscopic evolved gas analysis of **2b**.

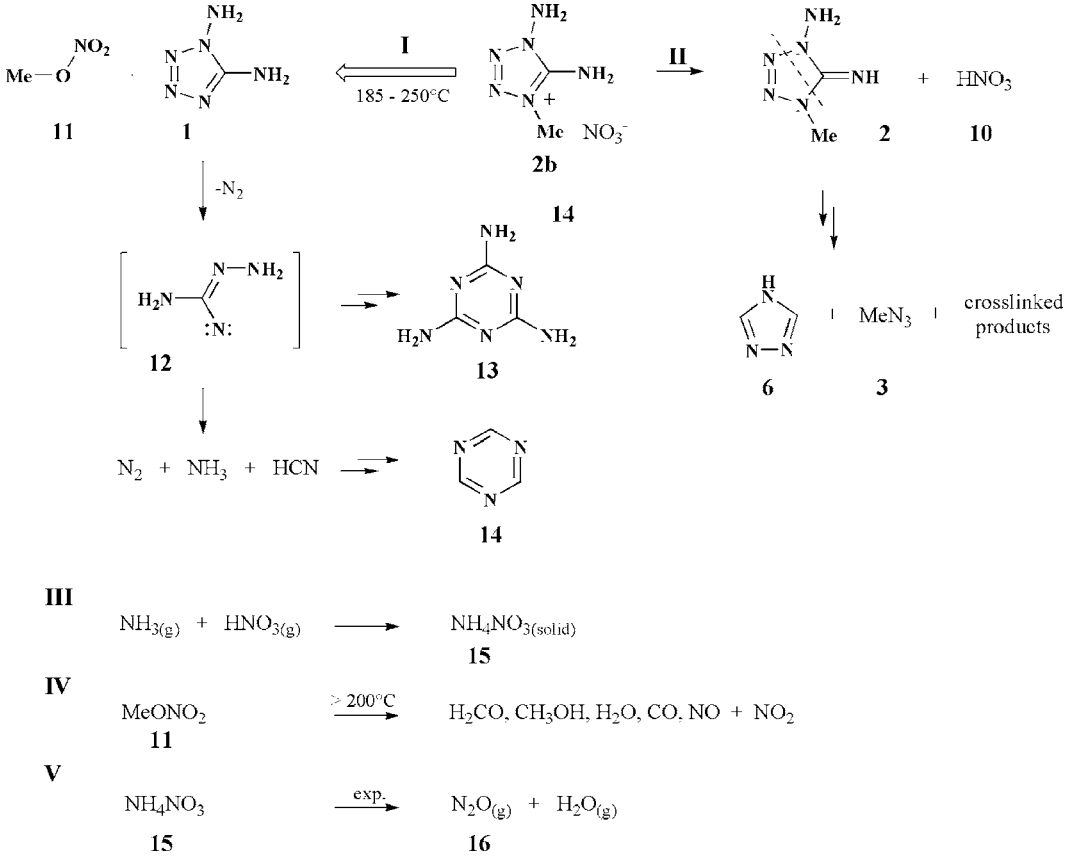

Scheme 2. Proposed decomposition pathway of **2b**.

mation of $MeONO_2$ (**11**) (*m*/*z* 46, no mass peak observed) and only as a minor process to the formation of HNO_3 (10, *m*/*z* 63) [43,44] (Scheme 2).

Compared to **2d** and AN, in the case of **2b** the main processes involves a methyl group transfer to **1** and methyl nitrate (**11**) and not a proton transfer to **10** (HN_3 in the case of **2d**) and **2** (Scheme 2, **I**). The main process observed is the formation of **11** (*m*/*z* 46, no mass peak observed) which was found to be the major product (Fig. 8) in the IR spectra of the

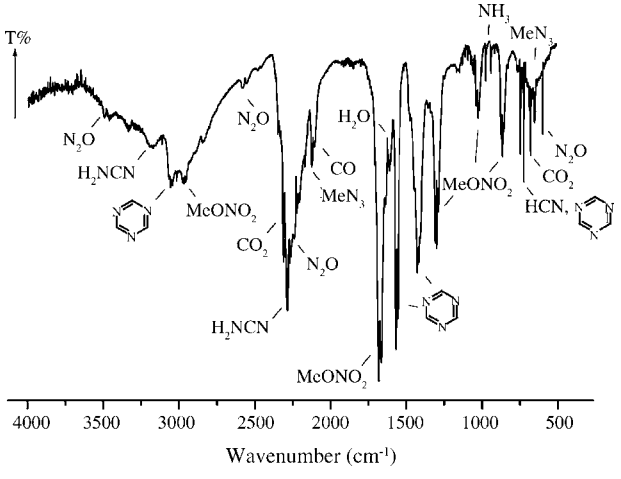

Fig. 8. Gas phase IR spectrum of the decomposition products of **2b**.

explosion products as well as in the spectra of the decomposition experiments and could also be identified in the mass spectrometry experiments (Fig. 9). Interestingly, under this reaction condition, the decomposition pathway discussed in [36], which involves the imino form of DAT (**1**), undergoes not the decomposition with the evolution of HN_3 (this was found in the case of **2d**), but rather eliminates nitrogen from DAT (**1**) (Scheme 2, **II**).

The resulting unstable nitrene (**12**) decomposes to HCN, NH_3 and N_2 according to Scheme 2 and in a minor process to cyanamide which is less stable and dimerizes to dicyandiamide that reacts through an intermediate to melamine (**13**) [34,45]. Cyanamide as gaseous product was also identified in the IR spectrum (Fig. 8) but in the gas phase cyanamide decomposes to NH_3, N_2 and HCN and was therefore not detected in the mass spectrum due to the hot ionic source.

The hydrogen cyanide undergoes in situ cyclotrimerization to the 1,3,5-triazine (**14**) (*m*/*z* 81, Fig. 9), which is known to proceed under harsh condition [46] and was also identified in the IR as well as mass spectrum (Figs. 8 and 9). In the case of **2b** only small amounts of MeN_3 indicates the partly decomposition of **2** according Scheme 2 (**II**) resulting from a proton transfer. Nitric acid and MeN_3 were found as components in the mass spectra of the residual explosion products in small quantities.

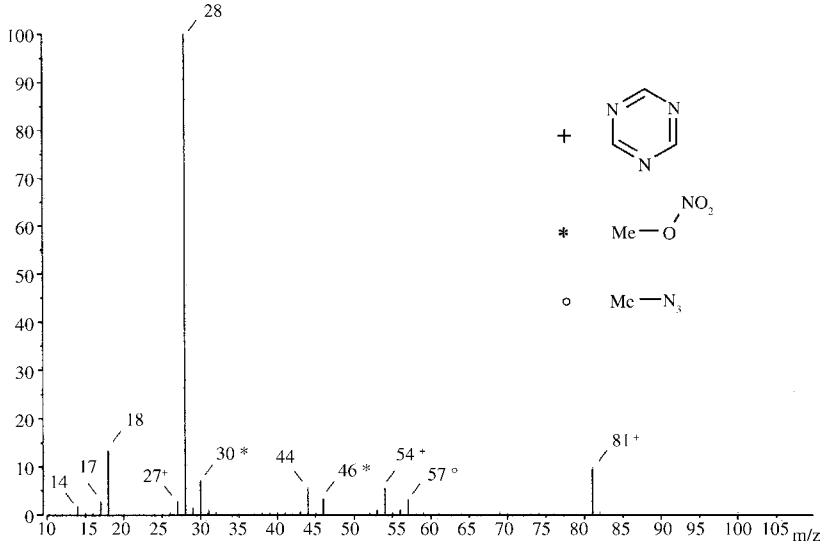

Fig. 9. Mass spectrum of the decomposition products of **2b**.

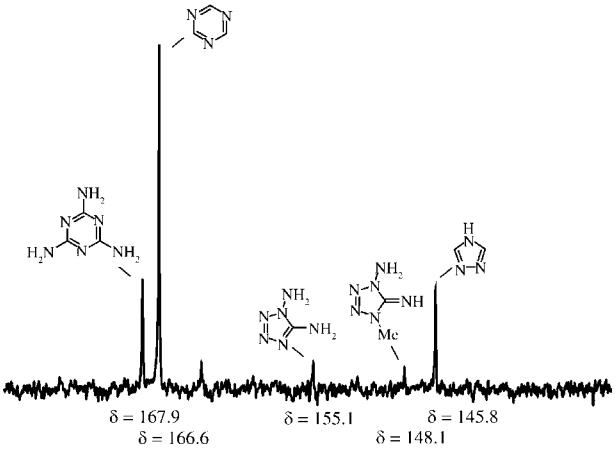

Fig. 10. ^{13}C-NMR spectra of decomposition products of **2b** recorded in [d6]-DMSO.

The 1,2,4-triazole (**6**), 1-amino-4-methyl-5-imino-4,5-dihydro-1*H*-tetrazole (**2**), 1,5-diamino-1*H*-tetrazole (**1**), 1,3,5-triazine (**14**) and melamine (**13**) could be identified by means of ^{13}C NMR spectroscopy (Fig. 10) and were found in the residue of the decomposition experiments. Ammonium nitrate (**15**), resulting from the recombination of HNO_3 and NH_3, was identified as one component of the obtained sublimate (Scheme 2, **III**) and explains the low concentration of ammonia. The thermal decomposition of **11** above 200 °C leads to the formation of CH_2O (*m*/*z* 30), CH_3OH (*m*/*z* 32), H_2O (*m*/*z* 18), CO (*m*/*z* 28), NO (*m*/*z* 30) and NO_2 (*m*/*z* 46) [47] (Scheme 2, **IV**).

The thermal decomposition of AN during explosion processes leads to the formation of N_2O (**16**) (*m*/*z* 44) and H_2O (*m*/*z* 16) and explains the occurrence of **16** in the IR spectrum (Scheme 2, **V**).

Compared to **2b**, **2c** (melting point 85 °C) shows a relatively stable melt up to ∼150 °C where shortly after, also in accordance with the DSC experiment, decomposition occurs

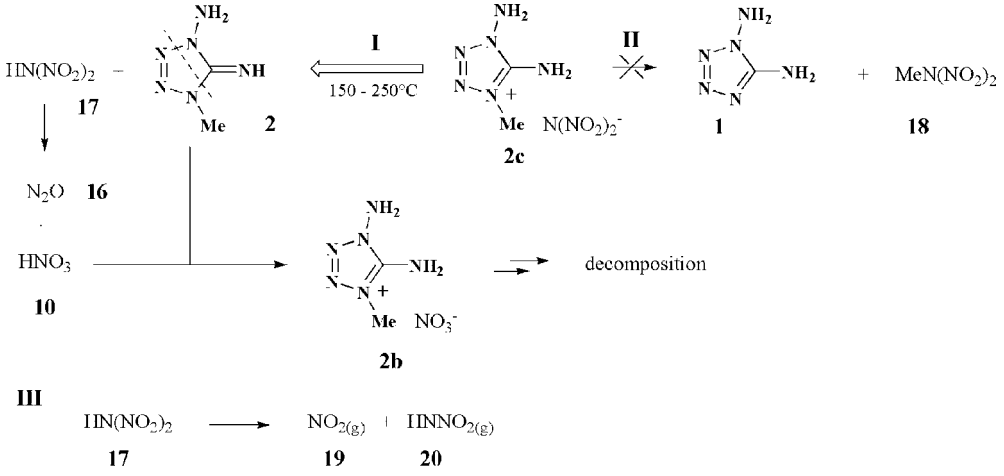

Scheme 3. Proposed decomposition pathway of **2c**.

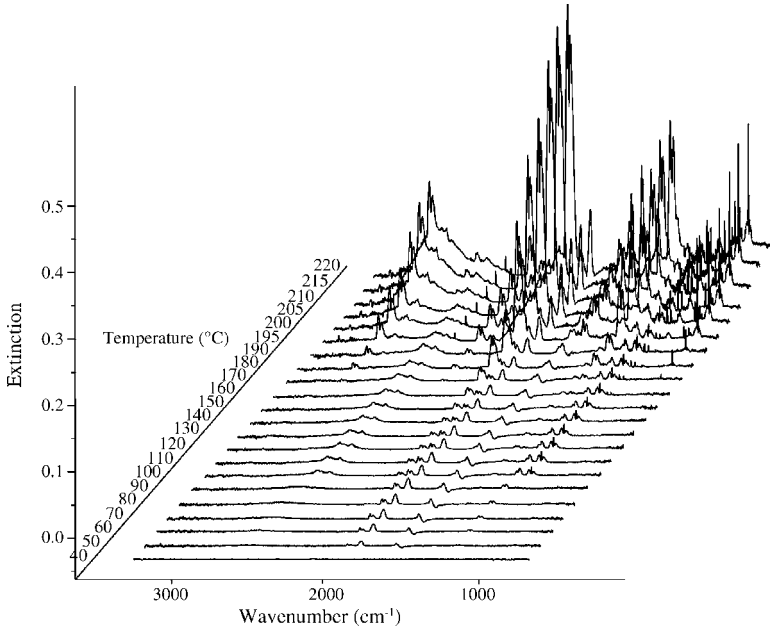

Fig. 11. Infrared spectroscopic evolved gas analysis of **2c**.

and a broad exothermic peak in the DSC and a sudden rise of gaseous products in the IR spectra indicates a spontaneous decomposition in one step. The thermal decomposition of **2c** under reduced pressure in the temperature range from 40 to 220 °C is depicted in Fig. 11.

Typical products observed during the decomposition of **2c** are N_2O (**16**) as the main product, MeN_3 (**3**), $MeONO_2$ (**11**), 1,3,5-triazine (**14**), HCN (**7**), NH_3 and H_2O (Fig. 12, Table 4).

The thermal decomposition is initiated by a proton transfer to subsequently produce dinitraminic acid HN_3O_4 (**17**) in the melt. According to [48], **17** decomposes under formation of N_2O (**16**) and HNO_3 which produce **2b** from the recombination of **2** and HNO_3. This reaction process is shown in Scheme 3 (**I**) and explains the obtained decomposition products which are similar to those of **2b**. No evidence, whether

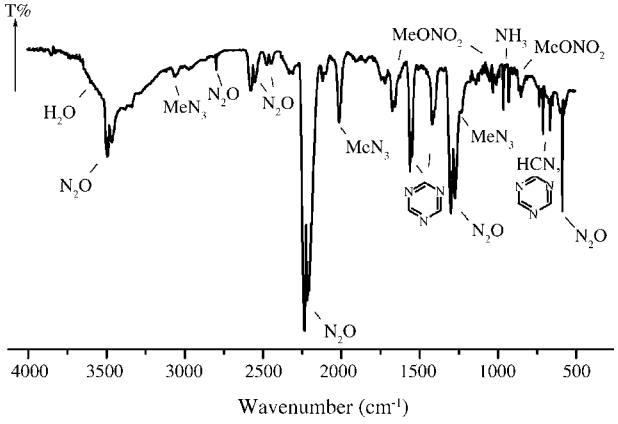

Fig. 12. Gas phase IR spectrum of the decomposition products of **2c**.

from the explosion experiments nor the decomposition experiments, was found for the formation of DAT (**1**) (Scheme 3, **II**) and methyldinitramide (**18**).

Interestingly, during the decomposition of **2c**, the formation of NO_2 was not observed which excludes the favored mechanism of decomposition of HN_3O_4 (**17**) to NO_2 (**19**) and $HNNO_2$ (**20**) according [11] at higher temperatures (Scheme 3, **III**).

4. Conclusion

The novel salts (**2b**, **2c** and **2d**) of 1-amino-4-methyl-5-imino-4,5-dihydro-1*H*-tetrazole (**2**) are new energetic materials with high nitrogen content. **2c** is very sensitive to friction but shows a reasonable stability toward impact. According the UN guideline ST/SG/AC.10/11 [34], **2c** is not safe for transport but prilling or putting on a binder of **2c** might increase the stability toward friction. The predicted detonation performance is higher than those found for RDX and the oxygen balance is in a reasonable limit. Therefore, **2c** might find application in liquid monopropellants, similar to HAN [56] and ADN [57] monopropellants. **2b** and **2c** are quite promising new materials too which might find application also as supplement in monopropellants (**2b**) or as a new promising material for gas generating mixtures (**2b**, **2c** and **2d**). All three compounds showing distinctive decomposition pathways which lead in the case of **2b** and **2c** to the same products and in the case of **2d** predominately to the formation of HN_3 and MeN_3. In all case, the major gaseous decomposition products are still highly endothermic compounds.

Acknowledgements

Financial support of this work by the University of Munich (LMU) and the Fonds der Chemischen Industrie is gratefully acknowledged (J.J.W. thanks for a FCI scholarship, DO 171/46). The authors are also indebted to and like to thank Mr. Gunnar Spieß for the drop hammer and friction tests. We are also indebted to and thank Mr. Christoph Rohbogner for his very valuable help concerning the preparation of the used compounds during his research project.

References

[1] D.E. Chavez, M.A. Hiskey, J. Energ. Mater. 17 (1999) 357.
[2] A. Hammerl, G. Holl, M. Kaiser, T.M. Klapötke, P. Mayer, H. Nöth, H. Piotrowski, M. Suter, Z. Naturforsch. 56b (2001) 857.
[3] A. Hammerl, G. Holl, T.M. Klapotke, P. Mayer, H. Noth, H. Piotrowski, M. Warchhold, Eur. J. Inorg. Chem. 4 (2002) 834.
[4] J. Geith, T.M. Klapötke, J. Weigand, G. Holl, Propellants, Explosives, Pyrotechnics 29 (1) (2004) 3.
[5] J.C. Bottaro, Chem Ind. 7 (1996) 249.
[6] N. Sikder, A.K. Sikder, N.R. Bulakh, B.R. Gandhe, J. Hazard. Mater. 113 (2004) 35.
[7] J. Hanks, T. Highsmith, A. Sanderson, K. Warner, J. Worthington, 33rd International Annual Conference of ICT, Karlsruhe, Germany, 2002, p. 129.
[8] B.T. Federoff, Encyclopedia of Explosives and Related Items, vol. 1, Picatinny Arsenal, New Jersey, 1960, pp. A311–A379.
[9] J.H. Koper, O.G. Jansen, P.J. Van den Berg, Explosivstoffe 8 (1970) 181.
[10] D.G. Patil, S.R. Jain, T.B. Brill, Propellants, Explosives, Pyrotechnics 17 (1992) 99.
[11] T.B. Brill, P.J. Brush, D.J. Patil, Combust. Flame 92 (1993) 178.
[12] K.O. Christe, W.W. Wilson, M.A. Petrie, H.H. Michels, J.C. Botttaro, R. Gilardi, Inorg. Chem. 35 (1996) 5068.
[13] R. Gilardi, J. Flippen-Anderson, C. George, R.J. Butcher, J. Am. Chem. Soc. 119 (1997) 9411.
[14] H. Östmark, U. Bemm, A. Langlet, R. Sandén, N. Wingborg, J. Energ. Mater. 18 (2000) 123.
[15] H. Östmark, U. Bemm, H. Bergman, A. Langlet, Thermochim. Acta 384 (2002) 253.
[16] A. How-Ghee, W. Fraenk, K. Karaghiosoff, T.M. Klapötke, P. Mayer, H. Nöth, J. Sprott, M. Warchhold, Z. Anorg. Allg. Chem. 628 (2002) 2894.
[17] I.B. Mishra, T.P. Russell, Thermochim. Acta 384 (2002) 47.
[18] H. Holfter, T.M. Klapötke, A. Schulz, Eur. J. Solid State 33 (1996) 855.
[19] T. Habereder, A. Hammerl, G. Holl, T.M. Klapötke, J. Knizek, H. Nöth, Eur. J. Inorg. Chem. 5 (1999) 849.
[20] A. Hammerl, G. Holl, M. Kaiser, T.M. Klapötke, R. Kränzle, M. Vogt, Z. Anorg. Allg. Chem. 628 (2002) 322.
[21] P.N. Gaponik, V.P. Karavai, Khim. Geterotsikl. Soedin (1984) 1388.
[22] G. Drake, T. Hawkins, AFRL/PRSP AFOSR Ionic Liquids Workshop, Tampa, FL, March 2004.
[23] V.E. Matulis, A.S. Lyakhov, P.N. Gaponik, S.V. Voitekhovich, O.A. Ivashkevich, J. Mol. Struct. 649 (2003) 309.
[24] T.M. Klapötke, P. Mayer, A. Schulz, J.J. Weigand, J. Am. Chem. Soc. 127 (2005) 2032.
[25] J.C. Gálvez-Ruiz, G. Holl, K. Karaghiosoff, T.M. Klapötke, K. Löhnwitz, P. Mayer, H. Nöth, K. Polborn, C.J. Rohbogner, M. Suter, J.J. Weigand, Inorg. Chem. 44 (12) (2005) 4237.
[26] Test methods according to the UN recommendations on the transport of dangerous goods, in: Manual of Tests and Criteria, fourth ed. (revised), United Nations Publication, New York\Geneva, 2003, ISBN 92-1-139087-7, Sales No. E.03.VIII.2, 13.4.2 Test 3(a)(ii) BAM Fallhammer.
[27] M.J. Kamlet, S.J. Jacobs, J. Chem. Phys. 48 (1968) 23.
[28] T. Ozawa, Bull. Chem. Soc. Jpn. 38 (1965) 1881.
[29] H.E. Kissinger, Anal. Chem. 29 (1957) 1702.
[30] Standard Test Methods for Arrhenius Kinetic Constants for Thermally Unstable Materials, ASTM designation E698-99, 1999.
[31] http://www.aist.go.jp/RIODB/SDBS/.
[32] C.L. Mader, Detonation Properties of Condensed Explosives Computed Using the Becker–Kistiakowsky–Wilson Equation of State, Los Alamos Scientific Laboratory, 1963. Rept. LA-2900.
[33] J. Köhler, R. Mayer, Explosivstoffe, 7 Aufl., Wiley-VCH, Weinheim, 1991.
[34] Recommendation on the transport of dangerous goods, in: Manual of Tests and Criteria, United Nations, New York/Geneva, 1995, ST/SG/AC.10/11 Rev.2, p. 74, 105.
[35] Standard Test Methods for Mol Percent Impurity by DSC, ASTM designation E928-996, 2003.
[36] C.E. Stoner, T.B. Brill, Combust. Flame 83 (1991) 302.
[37] L. Costa, G. Camino, J. Therm. Anal. 34 (1988) 423.
[38] S.V. Levchick, A.I. Balabanovich, O.A. Ivashkevich, A.I. Lesnikovich, P.N. Gaponik, L. Costa, Thermochim. Acta 225 (1993) 53.
[39] H. Behringer, H.J. Fischer, Chem. Ber. 95 (1962) 2546.
[40] A. Sapssov, E. Golovinsky, C. Demirov, Chem. Ber. 99 (1966) 3734.
[41] S.V. Levchick, A.I. Balabanovich, O.A. Ivashkevich, A.I. Lesnikovich, P.N. Gaponik, L. Costa, Thermochim. Acta 207 (1992) 115.
[42] B. Jurgens, E. Irran, J. Senker, P. Kroll, H. Muller, W. Schnick, J. Am. Chem. Soc. 125 (34) (2003) 10288.
[43] E. Kestila, M.E.E. Haju, J. Valkonen, Thermochim. Acta 214 (1993) 67.
[44] Y. Oyumi, T.B. Brill, J. Phys. Chem. 89 (1985) 4325.
[45] L. Gmelin, Gmelins Handbuch der anorgnischen Chemie, 8. Aufl., Verlag Chemie, Weinheim, 1971, Syst.Nr.14, Teil D1, p. 347.
[46] M.J.D. Low, P. Ramamurthy, J. Res. Inst. Catal. 16 (2) (1968) 535.
[47] S.R. Jain, M.V. Rao, V.R. Verneker, Propellants, Explosives, Pyrotechnics 3 (1979) 761.
[48] I.B. Mishra, T.P. Russell, Thermochim. Acta 384 (2002) 47.
[49] T. Shimanouchi, Tables of molecular vibrational frequencies consolidated volume II, J. Phys. Chem. Ref. Data 6 (3) (1972) 993.
[50] D.E. Milligan, M.E. Jacox, J. Chem. Phys. 56 (1975) 333.
[51] T. Shimanouchi, Tables of molecular vibrational frequencies consolidated, volume I, Natl. Stand. Ref. Data Ser., Natl. Bur. Stand. (1972) 1.
[52] C.D. Brand, T.M. Cawthon, J. Am. Chem. Soc. 77 (1955) 319.
[53] K. Nakamoto, Infrared and Raman Spectra of Inorganic and Coodination Compounds, fourth ed., Wiley & Sons, New York/Chichester/Brisbane/Toronto/Singapore, 1986.
[54] R. Mecke, F. Langenbucher, Infrared Spectra, Heyden & Son, London, 1965, serial no. 106.
[55] R. Mecke, F. Langenbucher, Infrared Spectra, Heyden & Son, London, 1965, serial no. 6.
[56] D. Meinhardt, G. Brewster, S. Christofferson, E.J. Wucherer, 34th AIAA/ASME/SAE/ASEE Joint Propulsion Conference, AIAA 98-4006, Cleveland, OH, USA, 13–15 July 1998.
[57] K. Anflo, T.A. Grönland, N. Wingborg, 36th AIAA/ASME/SAE/ASEE Joint Propulsion Conference, AIAA 2000-3162, Huntsville, AL, USA, 16–19 July 2000.